THE MEDIUM ENERGY COSMIC RAY EXPERIMENT FOR ISEE-C

T. T. von Rosenvinge, F. B. McDonald, J. H. Trainor,
M. A. I. Van Hillebeke & L. A. Fisk

Reprinted from IEEE Transactions on Geoscience Electronics, Vol. GE-16, No. 3, July 1978
0018-9413/78/0700-2085$00.75

The Medium Energy Cosmic Ray Experiment for ISEE-C

T. T. VON ROSENVINGE, F. B. McDONALD, J. H. TRAINOR, M. A. I. VAN HOLLEBEKE, AND L. A. FISK

Abstract—A description is provided of the medium energy cosmic ray experiment on board the ISEE-C spacecraft. This experiment is designed to measure the charge composition of nuclear energetic particles over wide ranges in energy (~1-500 MeV/nucleon) and in charge (Z = 1-28). Individual isotopes are resolvable for Z = 1-7 over a restricted energy range. Electrons of ~2-10 MeV are measured as well. These measurements are accomplished using all solid-state detector telescopes with detectors ranging in thickness from 15-3000 μm. The scientific goals of the experiment are also described. These include study of the composition of energetic particles from the sun and from the galaxy, the acceleration and flow of particles in the interplanetary medium, and electrons from Jupiter. Heliospheric gradients and other characteristics of solar modulation will be measured in conjunction with identical telescopes flown on the Voyager 1 and 2 spacecraft and similar telescopes on Pioneer 10 and 11.

I. INTRODUCTION

THE ENERGETIC particles observed in the interplanetary medium near Earth originate from a variety of sources which are being increasingly enumerated. In 1972, when the ISEE proposals were submitted to NASA headquarters, two main categories of particles were known: galactic and solar. In addition, very low energy (≤500-keV) particles had been observed to be coming from the Earth's magnetosphere. Since that time new classes of solar particle emissions have been discovered. For example, Hurford *et al.* [6] discovered ^{3}He-rich events in which the ratio ^{3}He/^{4}He sometimes exceeds 1 (as compared to the normal solar ratio of $\sim 2 \times 10^{-4}$). Unusual iron-rich events have also been discovered (e.g., [5]). Two new sources which have been identified include Jupiter (~3 - 10-MeV electrons [14] and the interplanetary medium itself [1], [7], and [9]). New populations of quiet-time particles have been identified for which the source (or sources) are not well known. For example, the quiet-time oxygen spectrum has been found to be anomalous at low energies [4] and to be such that the oxygen to carbon ratio between ~8 and 30 MeV/nucleon greatly exceeds the ratios observed for solar and galactic energetic particles [8]. The anomalous oxygen spectrum could be produced by acceleration in the solar wind as originally proposed by [2] (e.g., [11] and [15]). The connection between the anomalous oxygen spectrum and the anomalous He spectrum [3] is currently unclear, although both may have the same origin. McDonald *et al.* [10] have suggested a galactic origin for the anomalous He.

The discovery of new sources and new particle populations has resulted from a combination of increased detector resolution and sensitivity, exploration of the solar system by Pioneer 10 and 11, and by a return of the solar system since about 1972 to near solar-minimum conditions. To make further progress we have developed sensitive telescopes with excellent charge and energy resolution over extremely wide ranges of both parameters with mass resolution over more limited ranges. Extensive anisotropy measurements will be made as well. Descriptions of our very low energy telescopes (VLET's) and of our high energy telescopes (HET's) follow. The HET's are identical to telescopes being flown on Voyagers 1 and 2 which are currently headed for the outer solar system and beyond.

II. EXPERIMENT DESCRIPTION

This experiment consists of two pairs of telescopes referred to as the VLET's and the HET's. The combined charge, mass, and energy intervals covered by these telescopes are as follows:

1) Nuclei charge and energy spectra:
   Z = 1-30, energy range ~1-500 MeV/nucleon;
2) Isotopes: $Z = 1$, $\Delta M = 1$ from 4-70 MeV/n
   $Z = 2$, $\Delta M = 1$ from 1-70 MeV/n
   Z = 3-7, $\Delta M = 1$ from ~30-140 MeV/n;
3) Electrons: ~2-10 MeV;
4) Anisotropies: Z = 1-26 (1-150 MeV/nucleon for Z = 1, 2)
   Electrons (~2-10 MeV).

The VLET's and HET's are constructed wholly out of solid-state detectors, both the surface barrier and the lithium-drifted types. This choice is based primarily on their excellent resolution, long established reliability, and low weight. By using multiparameter analysis over the complete energy range, reducing pathlength variations through the use of curved dE/dx devices and minimizing Landau effects by choosing the thickest dE/dx device appropriate to a given energy interval, very great increases in telescope resolution and background rejection are realized. Both the HET and VLET systems operate in the self-calibrating dE/dx versus E mode where particle-track end points can be used to conclusively obtain absolute calibrations. There are two HET telescopes each mounted on the tower on the top of the spacecraft and there

Manuscript received April 3, 1978.

T. T. von Rosenvinge, F. B. McDonald, and J. H. Trainor are with the NASA Goddard Space Flight Center, Greenbelt, MD 20771.

M. A. I. Van Hollebeke is with the NASA Goddard Space Flight Center, Greenbelt, MD 20771 and the University of Maryland, College Park, MD 20742.

L. A. Fisk is with the University of New Hampshire, Durham, NH 03824.

0018-9413/78/0700-208$00.75 © 1978 IEEE

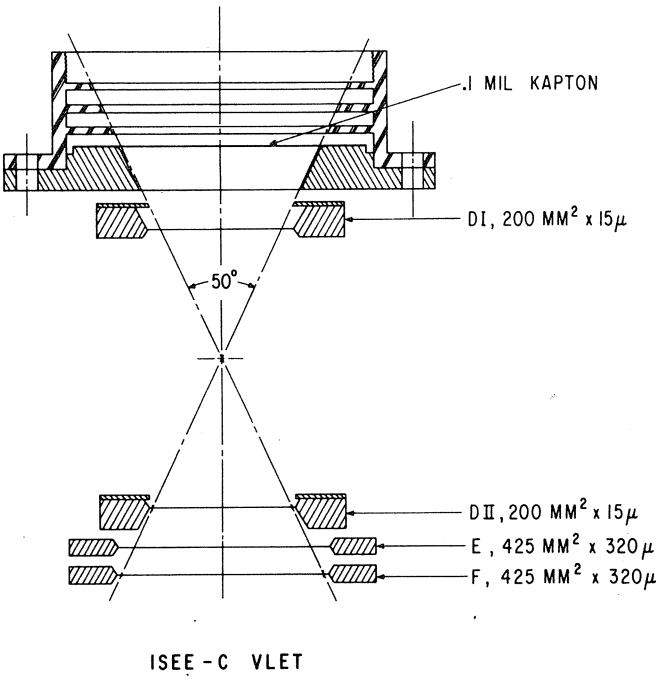

Fig. 1. Shows a schematic cross-sectional view of a VLET.

are two VLET telescopes looking out through spacecraft facet number 8. The HET and VLET systems are wholly independent of each other. The use of multiple telescopes and two independent systems provides increased reliability and geometry factor.

A. The Very Low Energy Telescope System

The Very Low Energy Telescope System is designed to measure the charge composition of low energy nuclei from hydrogen to iron. The energy range extends from ~2 MeV/nucleon (nearly independent of charge due to charge pick-up) to energies which overlap the low energy response of the HET system. ^{3}He is resolvable from ^{4}He from 1.3 to 7.9 MeV/nucleon. Fig. 1 is a schematic drawing of a single VLET telescope. The detector thicknesses, areas, and designations (DI, DII, E, and F) are also shown in Fig. 1. Each telescope has a geometry factor of 0.30 cm^2 sr. The thin (~0.5 mg/cm^2) foil in front of the detector stack is 0.1-mil Kapton twice aluminized on its inner surface (2350 Å) and coated with Si oxide (3700 Å) on its outer surface. This foil serves three functions: 1) to provide detector DI with thermal protection from the rocket fairing during launch and from solar heating after launch, 2) to prevent detector DI from detecting solar photons, and 3) to provide RF shielding from the spacecraft S-band transponder. Detector DI is so thin (~15 μ) that it has very little thermal mass and poor heat conduction to its edges, making it very heat sensitive. Each VLET has its symmetry axis lying in the spacecraft spin plane (nominally within ±1° of the ecliptic plane) and hence will view the sun once per spin, i.e., once every 3 s. Each VLET axis is tilted 15° with respect to a normal to facet 8 and in the direction of facet 7 in order to have a completely unobstructed field of view.

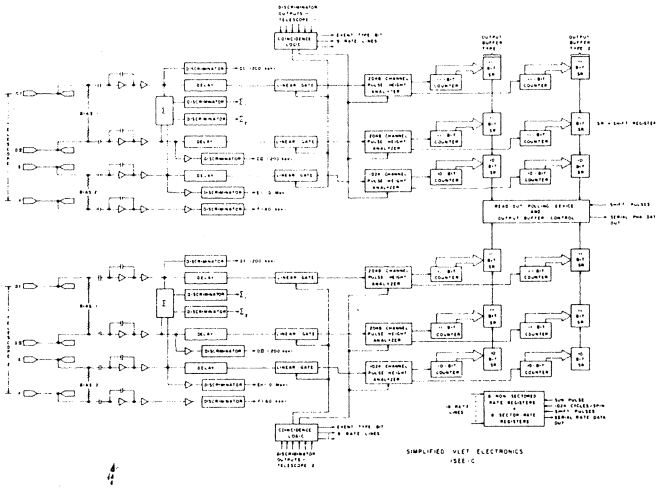

Fig. 2. A block diagram of the VLET electronics system.

Fig. 2 is a block diagram of the VLET electronics. The preamplifiers have been specially designed to have low noise (~75 keV) for the high detector capacitances of DI and DII (~1800 pF). Shaping time constants of 1 μ s and the use of bipolar pulses to minimize pulse pileup permit operation up to counting rates of at least 40 000 particles/s. Σ denotes a sum of pulses from the DI, DII, and E detectors which is discriminated at two levels, Σ_1 and Σ_2. Protons are unable to cause the Σ_1 level to be exceeded; helium nuclei cause the Σ_1 level to be exceeded but not the Σ_2 level; heavier nuclei exceed both levels. The electronics initiates pulse-height analysis for $Z > 1$ particles which penetrate the DI detector and come to rest in either the DII detector or in the E detector. Particles which enter the F detector are ignored. Two event types are identified by the coincidence conditions $DI \cdot DII \cdot \Sigma_1 \cdot \bar{F}$ ($Z = 2$) and $DI \cdot DII \cdot \Sigma_2 \cdot \bar{F}$ ($Z > 2$).

Observe in Fig. 2 that there is a set of pulse-height counters for each event type in each telescope. Each set has a corresponding output buffer (serial shift register). At any one time up to eight different events can be stored in the counters and output buffers waiting for readout. A read-out polling system automatically polls each output buffer in turn to see if it contains an event. If so, this event is read out into telemetry and the polling system then steps to the next output buffer. If an output buffer does not contain an event the polling system skips over it to the next output buffer to see if it contains an event. A null event is read out only if all the buffers are empty. This accumulation and readout system provides more efficient collection of heavy nuclei during times of high event rates than previous priority systems. Protons are not pulse-height analyzed but are rate analyzed. Protons and helium nuclei are both sectored in the spacecraft spin plane using 8 sector-rate counters.

An internal pulser system not shown in Fig. 2 can create events of each event type from each telescope for checking out the electronics system. A simple command system allows these internal pulsers to be turned on and off and also allows pulse-height analysis to be blocked for either telescope.

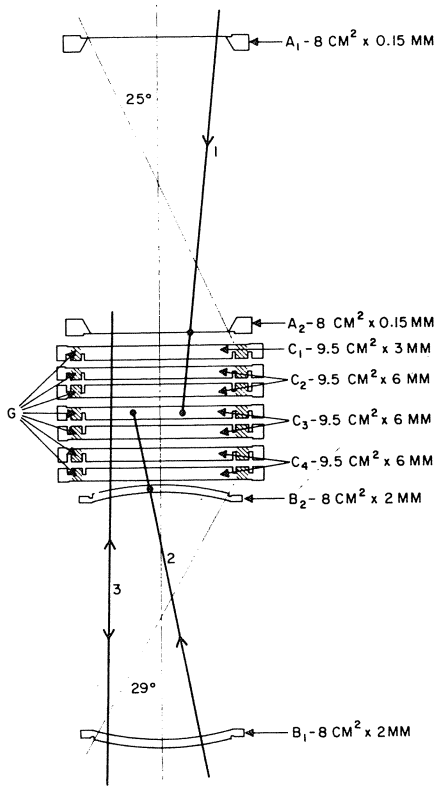

Fig. 3. A schematic cross-sectional view of a HET. Trajactories 1, 2, and 3 correspond to three different event types identified by the coincidence/anticoincidence logic.

The VLET system has been calibrated at the Rutgers/Bell 8 MV tandem Van de Graaff accelerator using beams of He^3, He^4, Li^6, C^{12}, O^{16}, and S^{32} and excellent resolution has been obtained.

The VLET system weighs 2.63 kg and consumes 2.1 W.

B. The High Energy Telescope System

The HET system is designed to measure the energy spectra of electrons and all elements from hydrogen to iron over a broad range of energies. Individual isotopes can be resolved up through the isotopes of nitrogen while individual charges are resolvable up through $Z = 26$. Fig. 3 is a schematic drawing of a single HET telescope. The detector thicknesses, areas, and designations ($A1$, $A2$, $B1$, $B2$, $C1$, $C2$, $C3$, $C4$, and G) are also shown in Fig. 3. $A1$ and $A2$ are thin (150-μ) surface barrier detectors, $B1$ and $B2$ are curved Li-drifted detectors and $C1$ through $C4$ are the central areas of double-grooved Li-drifted detectors. $B1$ and $B2$ are curved to minimize variations in path-length in these detectors due to the finite telescope opening angle [12]. The double grooves in the C detectors create annular detector rings around each central area. The annular detectors taken together constitute an anticoincidence or guard detector (denoted G) surrounding $C1$-$C4$. Accelerator tests indicate that cross talk between the central and annular areas is less than one part in 2 000. The G signal is discriminated at three different levels to prevent difficulties from this cross talk and also from knock-on electrons which may enter the guard.

TABLE I
HET SYSTEM PARAMETERS

EVENT TYPE	TYPE OF ANALYSIS	PROTON ENERGY RANGE (MeV)	SIMPLIFIED COINCIDENCE CONDITION	DETECTORS ANALYZED	GEOMETRY FACTOR (cm^2ster)	ACCEPTANCE ANGLE
A-Stopping	$\frac{dE}{dx}$ vs E	4-5	$A_1A_2\bar{C}_4\bar{G}$	A_1,A_2, $C_1+C_2+C_3$	0.8-1.2	50°
B-Stopping	$\frac{dE}{dx}$ vs E	18-70	$B_1B_2\bar{C}_1\bar{G}$	B_1,B_2, $C_2+C_3+C_4$	0.8-1.7	58°
Penetrating	TRIPLE dE/dx	70-500	$B_1B_2C_1$	B_1,C_1, $C_2+C_3+C_4$	1.7	46°

Each HET telescope is double ended with large acceptance angles at each end. In order that these acceptance angles be free from all obstructions, the HET's are mounted on the tower on the top of the spacecraft and with their symmetry axes lying in the spacecraft spinplane.

Three event types are recognized by the electronics, "*A*-Stopping," "*B*-Stopping," and "Penetrating" which correspond to trajectories 1, 2, and 3, respectively, in Fig. 3. These event types are further characterized in Table I.

Event type "*A*-stopping" represents particles which enter through A_1 and A_2 and stop before reaching C_4 or G. "*B*-stopping" events are particles which enter through B_1 and B_2 and stop before reaching C_1 or G. "Penetrating" particles penetrate B_1, B_2, and the complete C stack. The geometry factors cited in Table I are for a single telescope.

Fig. 4 presents a block diagram of the HET system. In order to accommodate the very wide dynamic range required for the HET electronics we have introduced a new element, a variable-gain charge-sensitive preamplifier. The preamplifier gain is electronically switched by an ultralow capacitance switch between high and low gain modes which differ in gain by factors from ~5 to ~10. In conjunction with the 4096 channel pulse-height analyzers, dynamic ranges of ~40 000 are then achievable. Fig. 4 shows that there are three 4096 channel pulse-height analyzers which are shared among the three different event types for each HET. The coincidence/anticoincidence logic and pulse summing have been designed so that pulse-height analysis can be performed without conflict from these multiple demands. The gains of C_1, C_2, C_3, and C_4, their gain change ratios, and their pulse-peaking times have been carefully matched so that a given amount of energy gives essentially the same $C_1 + C_2 + C_3$ or $C_2 + C_3 + C_4$ channel independently of how the energy is distributed among the three summed detectors.

In normal operation the two HET's will alternate between the high and low gain modes, switching gain once approximately every $8\frac{1}{2}$ min. In the high gain mode analysis will concentrate on electrons and nuclei with charge $Z = 1$-8 whereas in the low gain mode analysis will center on particles with charge greater than 2 and up to charge 26 (low gain "*B*-Stopping" and "Penetrating" events include charge 2 while low gain "*A*-Stopping" does not). Fig. 4 illustrates in part how electrons and nuclei with $Z = 1$, $Z = 2$, and $Z > 2$ are electronically differentiated. For example, a linear analog sum of the B_1, B_2, C_2, C_3, and C_4 pulses is threshold discriminated to produce logic pulse *SB*. In high gain the *SB* threshold cannot be exceeded by electrons and penetrating protons but can be exceeded by stopping nuclei with $Z \geqslant 1$.

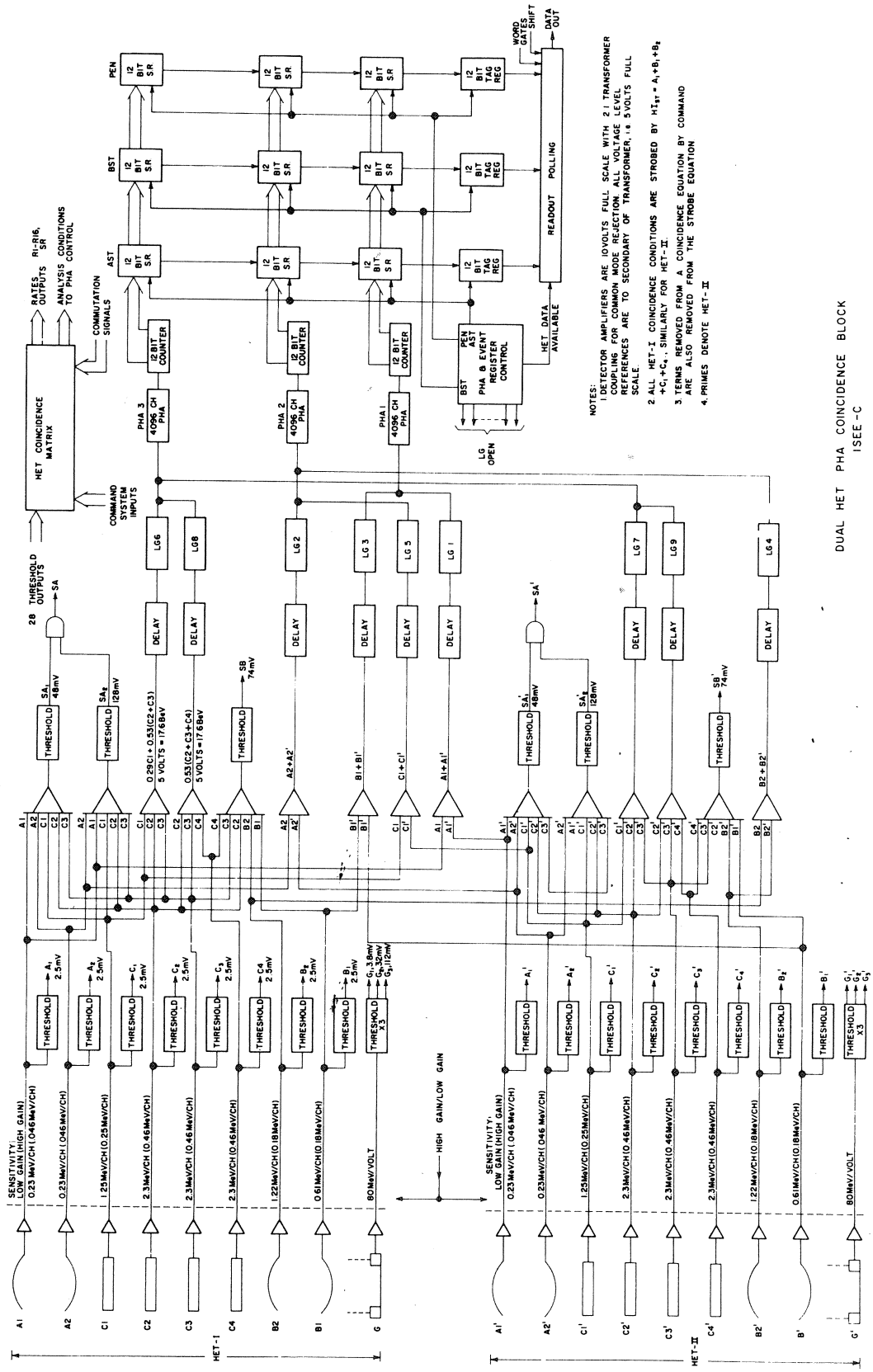

Fig. 4. A block diagram of the HET electronics system.

In low gain $Z \geqslant 2$ nuclei can trigger *SB*. *SA* is used only in low gain and can be produced only by particles with charge $Z > 2$. *SA* and *SB* are used in many of the rate equations in addition to being used to define the different event types.

The HET electronics has a polling system for reading out pulse-height data which is similar to that for the VLET. As shown in Fig. 4, there is a read-out buffer for each of the three event types. These buffers are shared between the two HET's.

Anisotropies will be measured in two complementary ways. In each case the data is divided into eight parts (sectored) according to which octant in the ecliptic plane the telescope axes are pointing. Each pulse-height-analysis readout is tagged with three octant-identifier bits. This allows sectoring during quiet times with the possibility of rejecting background events (usually isotropic) on the basis of pulse heights. This permits measurement of much smaller anisotropies (~0.1 percent) than is otherwise possible. During solar active times, when particles enter a telescope faster than they can be read out in telemetry, anisotropies cannot be measured in this way [13]. It is then necessary to sector rates. Generally at these times background events are negligible and anisotropies are larger than at quiet times so that sectoring rates is appropriate. Electrons, protons, and helium nuclei will be rate sectored. During quiet times anisotropies may be measured up to approximately twice the end-point energy. Above this energy particles moving forward through the telescope cannot be distinguished from backward moving particles so that anisotropies are no longer measurable.

A complex command system allows various preamplifiers to be turned off, terms to be deleted from coincidence/anticoincidence equations, setting of fixed gain modes, and deletion of pulse-height readout for each event type. This capability is provided primarily for the event that certain detectors become noisy in space or in case other failures occur. When powered on the experiment automatically comes on in a nominal mode which preferably will not have to be changed.

The HET system has been calibrated at the Lawrence Radiation Laboratory Bevalac using beams of Fe^{56}, N^{15}, and nuclear fragments from these elements. As a result some changes were made in the digital logic to improve cross-talk rejection.

The HET system weighs 4.38 kg and consumes 3.1 W.

C. The Experiment Ground Support Equipment

The experiment ground support equipment will be briefly described here since it contained several features which were particularly helpful. It consisted of an Interdata 7/16 minicomputer, an 800 BPI magnetic tape drive, two CRT terminals (one for displaying data, one as control terminal), a dual magnetic disk drive, a Textronix 4006 display for displaying two-dimensional pulse-height matrices and histograms, a Versatec printer, and a CAMAC crate. The CAMAC crate contained a spacecraft simulator module, a computer controllable clock, DAC and routing matrix for driving pulsers to test either experiment, and a spacecraft-data frame synchronizer. An important aspect of the spacecraft simulator is that it normally formats the experiment data into a serial bit-stream identical to that from the spacecraft. Thus all the data display facilities are available whether the experiment is in the spacecraft or on the bench. This is useful, since the spacecraft test computer is only able to display data from one experiment at a time. An accelerated format and bit-rates up to 16 kbit/s are also available for gathering and displaying data during accelerator testing. Post-launch quick-look data can be processed on the same machine as well.

Acknowledgment

The HET and VLET systems were designed, built, and tested in parallel with an unprecedented number of other projects. This called for assistance from a much larger number of individuals at various times than would normally be the case. We thank all of the following for playing their parts: W. D. Davis (Lead Engineer; responsible for all solid-state detectors and VLET); C. H. Ehrmann (GSE Engineer); R. H. Hoffman (Thermal Engineer); G. Porreca (VLET Engineer); D. E. Stilwell and R. M. Joyce (HET Engineers); H. E. Trexel (Mechanical System Design, HET, and VLET); H. D. White (Data Processing Unit Engineer); and Technicians M. Powers (VLET) and M. Beazley, F. Birsa, and M. Noordzy (HET). Spacetac, Incorporated produced most of the electronics for both HET and VLET. Surface barrier detectors were obtained from Ortec, Inc. and Li-drifted detectors were obtained from the Kevex Corporation. A. Engel of the Computer Sciences Corporation was responsible for the GSE software effort. W. Slemp of the Materials Division of NASA Langley Research Center provided the thin foils for the VLET. These foils were coated at NASA Goddard Space Flight Center under the direction of J. Triola. Accelerator time and generous support were provided by the staff of the Bevalac at the Lawrence Berkeley Radiation Laboratory and by the staff of the Rutgers/Bell 8 MV tandem Van de Graaff accelerator. Finally, support from the ISEE Project Office and from Fairchild Space and Electronics Company are gratefully acknowledged.

References

[1] C. W. Barnes and J. A. Simpson, *Ap. J. (Lett.)*, vol. 210, p. L91, 1976.
[2] L. A. Fisk, B. Kozlovsky, and R. Ramaty, *Ap. J. (Lett.)*, vol. 190, p. L35, 1974.
[3] M. Garcia-Munoz, G. M. Mason, and J. A. Simpson, *Ap. J. (Lett.)*, vol. 182, p. L81, 1973.
[4] D. Hovestadt, O. Vollmer, G. Gloeckler, and C. Y. Fan, *Phys. Rev. (Lett.)*, vol. 31, p. 650, 1973.
[5] D. Hovestadt, B. Klecker, O. Vollmer, G. Gloeckler, and C. Y. Fan, in *14th Int. Cosmic Ray Conf.* vol. 5, p. 1613, 1975.
[6] G. J. Hurford, R. A. Mewaldt, E. C. Stone, and R. E. Vogt, *Ap. J. (Lett.)*, vol. 201, p. L95, 1975.
[7] F. E. Marshall, and E. C. Stone, *Geophysics Res. Lett.*, vol. 4, p. 57, 1977.
[8] F. B. McDonald, B. J. Teegarden, J. H. Trainor, and W. R. Webber, *Ap. J. (Lett.)*, vol. 187, p. L105, 1974.
[9] F. B. McDonald, B. J. Teegarden, J. H. Trainor, T. T. von Rosenvinge, and W. R. Webber, *Ap. J. (Lett.)*, vol. 203, p. L149, 1976.
[10] F. B. McDonald, N. Lal, J. H. Trainor, M. A. I. Van Hollebeke, and W. R. Webber, *Ap. J. (Lett.)*, vol. 216, p. 930, 1977.
[11] R. B. McKibben, *Ap. J. (Lett.)*, vol. 217, p. L113, 1977.
[12] M. A. Perkins, J. J. Kristoff, G. M. Mason, and J. D. Sullivan, *Nuclear Inst. and Meth.*, vol. 68, p. 149, 1969.
[13] E. C. Roelof, *J. of Geophys. Res.*-vol. 79, p. 1535, 1974.
[14] B. J. Teegarden, F. B. McDonald, J. H. Trainor, W. R. Webber, and E. C. Roelof, *J. Geophys. Res.*-vol. 79, p. 3615, 1974.
[15] T. T. von Rosenvinge, and F. B. McDonald, in *14th Int. Cosmic Ray Conf. Proc.*, vol. 2, p. 792, 1975.